



Experimental investigation of trioctahedral micas in the Na₂O-FeO-Fe₂O₃-Al₂O₃-SiO₂-H₂O-HF system

*Boubker Boukili¹, Nacir El Moutaouakkil¹, Jean-Louis Robert²,
Alain Meunier³ and Giancarlo Della Ventura⁴

¹LO3G, Faculty of Sciences, University Mohammed V, BP 1014-Rabat, Morocco.

²IMPMC 4, University of Pierre and Marie Curie, Place Jussieu, 75005 Paris, France.

³UFR SFA-IC2MP, University of Poitiers, Bâtiment B35, Poitiers Cedex 9, France.

⁴Department of Geological Sciences, University of Roma Tre, I-00146 Roma, Italy.

Received 17 Nov 2014, Revised 20 Oct 2015, Accepted 30 Oct 2015

*Corresponding author: E-mail: boubkerboukili@gmail.com

Abstract

The purpose of this work is to explore the solid solution and stability of trioctahedral micas in the system: Na₂O-FeO-Fe₂O₃-Al₂O₃-SiO₂-H₂O-HF. Synthesis were carried out in cold-seal pressure vessels, at 600°C, 1kbar PH₂O, under fO₂ conditions set by NNO and MW buffers. Starting compositions belong to the annite - siderophyllite join and can be expressed as Na(Fe_{3-x}Al_x)(Si_{3-x}Al_{1+x})O₁₀(OH,F)₂, where x represents the extent of the Tschermark-type substitution. In the F-free system, under the NNO buffer, the Na-annite(OH) (x = 0) composition produced a two phase assemblage albite + magnetite. Along the join, in the 0.5 ≤ x ≤ 1 compositional range, hydrated mica is found to coexist with minor amounts of hercynite and a silicate, possibly analcime. Powder XRD shows the presence of three hydration states (2W: two water layers, 1W: one-layer water and 0W: anhydrous state) whose proportions depend on the bulk aluminum content in the system. Virtually the same results are obtained using the MW buffer. The starting composition corresponding to the Na-annite(OH) produced fayalite and albite, while Al-rich compositions gave hydrated micas with 2W and 1W hydration states; anhydrous mica occurs in very weak amounts. FTIR spectroscopy in the OH-stretching region of the hydrated micas indicates a high trioctahedral character. Experiments carried out in F-bearing system gave micas with high proportions of anhydrous state (0W). At the starting composition of Na-annite (F), a mica associated with minor magnetite and quartz is produced. Na-Al annite(F) (x = 0.5) is obtained as a pure anhydrous. It's one of the most promising compounds obtained in this study.

Keywords: Na-annite, Na-Al annite(F), Na-siderophyllite, hydrates, fluorine, FTIR spectroscopy.

1. Introduction

Biotites are ubiquitous minerals occurring in different geological environments. Their composition varies in a complex solid solutions domain due to a wide range of cationic and anionic substitution within the crystal structure [1]. Dymek [2] has identified fifteen theoretical mechanisms of ionic substitutions that may operate alone or simultaneously during the crystallization. The biotite interlayer sites may host K⁺, Na⁺, Ca²⁺, Ba²⁺, H₃O⁺, vacancies, and, more rarely Rb⁺, Cs⁺, Sr²⁺, and NH₄⁺. In natural systems, sodium is the second occupant of the interlayer sites after potassium; its content may reach up to 20% of the alkali site in micas from igneous rocks [3] while higher contents (from 32 to 97%) have been described by [4] in some biotites with numerous interlayer vacancies.

Although uncommon, Mg-rich trioctahedral sodic micas are increasingly described in the mineralogical literature. They have been reported as inclusions and/or accessory phases in anhydrous minerals (garnets and chromites) from ophiolitic sequences, where Na-phlogopite coexists with pargasite [5-8]. Al-rich members were found associated with Al-pargasite and zoisite within metamorphosed mafic and ultramafic complexes [9] and eclogitic retro-morphosed rocks [10-12]. Similarly, Na-bearing biotites are not common. They have been described in pelitic schists of the amphibolite facies [13] and metadikes from the Malàguide Complex [14].

Wonesite - $(\text{Na,K})_{0.5}(\text{Mg,Fe,Al})_3(\text{Si,Al})_4\text{O}_{10}(\text{OH,F})_2$ - has been discovered in Post Pond Volcanics [15; 16]; this Na-rich mica contains some Fe ions and exhibits a significant degree of Al-Tschermak substitution.

Natural Na-ferrous-rich biotites have not been reported in literature so far, in agreement with experimental work [17-20] suggesting a stability field for Fe-rich Na-micas much smaller than for their magnesium equivalents. Earlier investigation performed by [21] reported the synthesis of Na-annite(OH) end-member, and later studies [22; 23] indeed suggested that vermiculite, misinterpreted as a weathering or retrograde products of biotites, may be in fact the hydrated forms of Na-trioctahedral micaceous phases.

The interest to investigate in more details this sodic micas system originates from the contradictions emerged during the above mentioned works and from the need to provide further data regarding the effect of the $\text{OH} \rightarrow \text{F}$ substitution at the anionic site [24-30]. In this work we address the experimental investigation of trioctahedral micas in the system: $\text{Na}_2\text{O}-\text{FeO}-\text{Fe}_2\text{O}_3-\text{Al}_2\text{O}_3-\text{SiO}_2-\text{H}_2\text{O}-\text{HF}$, along the nominal Na-annite $[\text{Na}(\text{Fe}^{2+})_3(\text{Si}_3\text{Al})\text{O}_{10}(\text{OH,F})_2]$ -Na-siderophyllite $[\text{Na}(\text{Fe}^{2+})_2\text{Al}(\text{Si}_2\text{Al}_2)\text{O}_{10}(\text{OH,F})_2]$ join. Experiments were carried out under hydrothermal conditions and oxygen fugacity controlled by NNO and MW buffers. The run products were characterized by combining X-ray diffraction and FTIR spectrometry. We stress that understanding the crystal-chemical properties of these trioctahedral micas, particularly in F-bearing systems, is of interest from both geologic and applied point of view. As a matter of fact, fluorine is frequently involved in mineralization processes where micas are involved both as primary and as secondary phases [31-35]. From the view point of applications in environmental mineralogy, the hydrated phyllosilicates are often cited for their properties of fluorine, metals and organic molecules removal from solutions [e.g., 24; 25; 36; 37]

2. Experimental methods and analytical procedures

The synthesis and characterization of the products were performed in CRSCM-CNRS, Orléans, France. Gels prepared according to the method of [38] were used as starting materials for the hydrothermal syntheses. Sodium was introduced as dry Na_2CO_3 , silicon as tetraethylorthosilicate (TEOS) while aluminum and part of iron (50%) as nitrate. Finally, fluorides (AlF_3 or FeF_2) and metallic iron (50%) were mechanically added to the gels in order to obtain the appropriate stoichiometry. The compositions of trioctahedral micas studied are presented using to the half formula-unit formalism: $\text{Na}(\text{Fe}_{3-x}\text{Al}_x)(\text{Si}_{3-x}\text{Al}_{1+x})\text{O}_{10}(\text{OH})_2$ and $\text{Na}(\text{Fe}_{3-x}\text{Al}_x)(\text{Si}_{3-x}\text{Al}_{1+x})\text{O}_{10}(\text{F})_2$, for the F-free and F-bearing systems respectively, where x corresponds to the extent of the Al Tschermak-type substitution.

The following terminology will be used throughout the text: Na-annite and Na-siderophyllite referring to compositions with x equal to 0 and 1, respectively. These compositions are the sodium equivalents of annite and siderophyllite end-members given in the IMA approved classification scheme of micas [39]. We will use Na-Al annite to designate the composition with x = 0.5 (nominally). Consequently, in the following, the term Na-Al annite corresponds to a ferro-aluminous intermediate composition with ideal stoichiometry $\text{Na}(\text{Fe}_{2.5}\text{Al}_{0.5})(\text{Si}_{2.5}\text{Al}_{1.5})\text{O}_{10}(\text{OH,F})_2$.

Syntheses were performed in a Tuttle-type externally heated pressure vessels working vertically, with water as the pressure medium. Temperature was measured using K-type thermocouples calibrated against the melting points of NaCl and ZnCl_2 . The uncertainty is lower than $\pm 5^\circ\text{C}$. Pressure was measured using a Bourdon manometer, with an uncertainty of less than ± 50 bars. Experiments were performed at 600°C , 1 kbar PH_2O , with duration of 7 days. The choice of temperature and redox conditions was made from the results of the pioneering experimental works on the stability of K-trioctahedral micas [40; 41]. The duration was chosen to be compatible with the lifetime of the fO_2 buffers used here to yield a reproducible equilibrium in synthetic samples. The oxygen fugacity was controlled by the double capsule method of [42], using the magnetite-wüstite (MW) and the nickel-nickel oxide (NNO) assemblages as solid buffers introduced with water in an external Au-capsule. Gels were introduced the inner capsule ($\text{Ag}_{70}\text{Pd}_{30}$), with 15 wt% distilled water. Cooling was operated by removing the vessel from the furnace in order that a temperature lower than 100°C is reached after 1 hour.

The run products were examined using an optical microscope and a scanning electron microscope (SEM Philips Co.) equipped with an energy dispersive analyzer (EDS). Some micas were analyzed qualitatively to check the composition. X-ray diffraction patterns were obtained in the $5^\circ \leq 2\theta \leq 65^\circ$ angular range using the Co-K α ($\lambda = 1.79021 \text{ \AA}$) radiation. The d_{060} interplanar distances were measured using Si as an internal standard.

Infrared spectra were collected at room temperatures using a Nicolet 710 spectrometer. Samples were prepared as KBr pellets, with a mineral to KBr ratio of 5% and 0.2% for measurements in the high frequency ($3800-3200 \text{ cm}^{-1}$) and the low-frequency range ($1200-400 \text{ cm}^{-1}$), respectively. Compressed discs were kept overnight at 150°C to minimize the amount of adsorbed moisture. Each sample was scanned 64 times with a nominal resolution of 2 cm^{-1} . Spectra were decomposed using the PeakFit© program. A Lorentzian peak shape was used to model all components although minor deviations between raw and fitted spectra were observed toward the higher wavenumber side of N-bands [e.g. 43]; this is due to the

Christianssen effect [44]. The band nomenclature of [45-47] was adopted for the description of the infrared spectra in the OH-stretching vibration range (3800-3200 cm⁻¹).

3. Experimental results and discussion

3.1. F-free NNO buffered experiments

The phase assemblages obtained are listed in Table 1. The Na-annite (x = 0) starting composition did not yield any phyllosilicate phase but only albite and magnetite. A poorly crystallized hydrated sodium mica is obtained in the 0.2 ≤ x ≤ 0.4 composition range, together with magnetite and albite. The product is massive with a “cauliflower” appearance; the crystal size of the mica platelets is lower than 2 μm. The crystallites do not exhibit any pseudo-hexagonal shape. XRD powder patterns, acquired under humid atmosphere (Fig. 1), show the presence of mica with no water (W0, see [48]) and two water molecules in the interlayer regions (W2), characterized by basal d₀₀₁ spacings of ~ 9.7 Å and ~14.8 Å respectively [48]. The intensities of the 001 peaks are approximately equal. Compared to the 001 diffraction peak at 9.65 Å, the intensities of the 4.62 Å/002, 3.224 Å/003, 2.664 Å/200, 2.494 Å/-132, 2.224 Å/-133 and 1.457 Å/-206 ones are 15%, 80%, 50%, 40%, 30%, and 30% respectively, in agreement with data reported for Al-rich K-annite(OH) synthesized by [41]. It is to be noticed that here, and for other XRD patterns discussed in the text, the diffraction peaks were indexed in comparison with the published data of potassic equivalents [e.g.49; 50].

Table 1: Experimental products obtained at 600°C, NNO buffer and 1kbar along the join Na-annite-siderophyllite(OH). (*) denotes experimental results of [20] obtained at 500°C, NNO buffer and 5kbar. Interplanar distances d₀₆₀ are measured at ±0.004 Å. 2W, 1W, 0W and d-spacing refer to hydrates described by [48]. The phases encountered are hydrated mica <mc>, magnetite <Mag>, albite <Ab>, hercynite <Hcy>, analcime <Anl>, expansible ordered mixed layer <eml>. Brackets (..), indicate accessories phase, ((..)) trace amount.

Starting composition	Phases obtained	Hydrates (Å)
Present study (Na)(Fe ₃)(Si ₃ Al ₁)O ₁₀ (OH) ₂ (Na)(Fe _{2.9} Al _{0.1})(Si _{2.9} Al _{1.1})O ₁₀ (OH) ₂	Ab + Mag Ab + Mag + ((mc))	- 0W = 9.788
(Na)(Fe _{2.8} Al _{0.2})(Si _{2.8} Al _{1.2})O ₁₀ (OH) ₂ (Na)(Fe _{2.7} Al _{0.3})(Si _{2.7} Al _{1.3})O ₁₀ (OH) ₂	Ab + (mc) + Hcy Ab + (mc) + Hcy	2W = 14.768 - 0W = 9.788 2W = 14.898 1W = 12.397 0W = 9.788
(Na)(Fe _{2.6} Al _{0.4})(Si _{2.6} Al _{1.4})O ₁₀ (OH) ₂ (Na)(Fe _{2.5} Al _{0.5})(Si _{2.5} Al _{1.5})O ₁₀ (OH) ₂	(Ab) + mc + Hcy ((Ab)) + mc + Hcy	2W = 14.828 1W = 12.294 0W = 9.724 2W = 15.021 1W = 12.339 0W = 9.707
(Na)(Fe _{2.4} Al _{0.6})(Si _{2.4} Al _{1.6})O ₁₀ (OH) ₂ (Na)(Fe _{2.3} Al _{0.7})(Si _{2.3} Al _{1.7})O ₁₀ (OH) ₂	mc + Hcy + ((Anl)) mc + Hcy + ((Anl))	2W = 14.76 1W = 12.391 0W = 9.792 2W = 15.021 1W = 12.294 0W = 9.724
(Na)(Fe _{2.2} Al _{0.8})(Si _{2.2} Al _{1.8})O ₁₀ (OH) ₂ (Na)(Fe ₂ Al ₁)(Si ₂ Al ₂)O ₁₀ (OH) ₂	mc + (Hcy) mc + (Hcy)	2W = 14.891 1W = 12.339 0W = 9.792 - 1W = 12.294 0W = 9.788
Results from [20] * (Na)(Fe ₃)(Si ₃ Al ₁)O ₁₀ (OH) ₂ * (Na)(Fe _{2.5} Al _{0.5})(Si _{2.5} Al _{1.5})O ₁₀ (OH) ₂	Ab + Mag Pg + Ab + Mag + eml	-

The very weak peak at ~ 7.40 Å (Fig. 1) corresponds to the 002 reflection of a two-water layer (2W). The runs with 0.5 ≤ x ≤ 1 starting composition yielded hydrated mica with minor hercynite, and an additional silicate, possibly analcime (Table 1). SEM pictures clearly reveal the presence of pseudo-hexagonal flakes typical of the mica morphology with a mean crystal size of 2-3 μm (Fig. 2). EDS spectra (Fig. 3) suggest that the hydrated-mica compositions do not significantly deviate from the ideal stoichiometry. The mica phases exhibit (Fig. 1) the three hydrated states described by [48] characterized by d₀₀₁ spacings at ~14.8 Å, ~12.3 Å and ~9.7 Å which are typical of two-layer (2W), one-layer (1W) and dehydrated (0W) layer states, respectively.

Powder XRD patterns show an intense 001 and higher-order (00*l*) reflections of the anhydrous state. However, for the nominally Na-siderophyllite(OH) end-member composition (Fig. 1 top), the predominant state of the mica product is one-layer water with interplanar spacing at 12.29 Å. A small amount of anhydrous mica with a *c* parameter of 9.78 Å has been detected. The reflection at 7.40 Å is very weak and vanishes as the proportion of two-layer hydrate units decreases. The measured interplanar distances $d_{060} = \sim 1.548$ Å (Table 1), suggests a trioctahedral character of the hydrated micas. It decreases with increasing *x*-value (from ~ 1.56 Å to 1.54 Å) as shown by [51, 50, 47]. Furthermore, our findings are consistent with the studies of [20] who did not obtain a pure mica phase product.

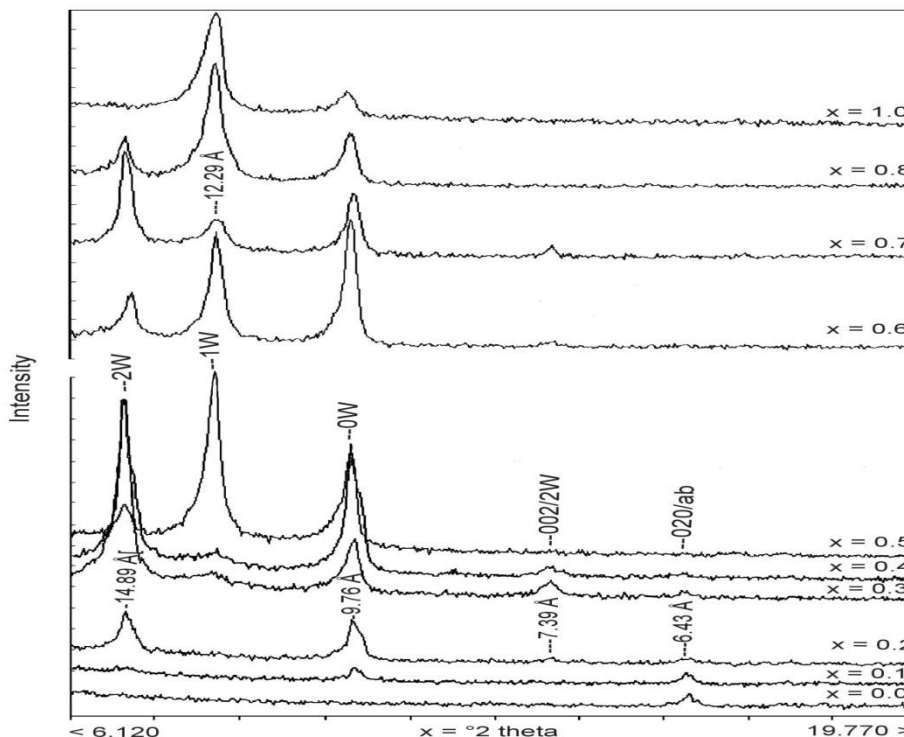


Figure 1: XRD patterns of hydrated micas acquired in conditions of atmospheric humidity. The numbers: 2W, 1W and 0W indicate the hydrate degree. Three hydration states are observed (2W, 1W and 0W). The diffraction peak at 6.43 Å belongs to (020) plan of albite. *x* corresponds to the amount of the Tschermak-type substitution.

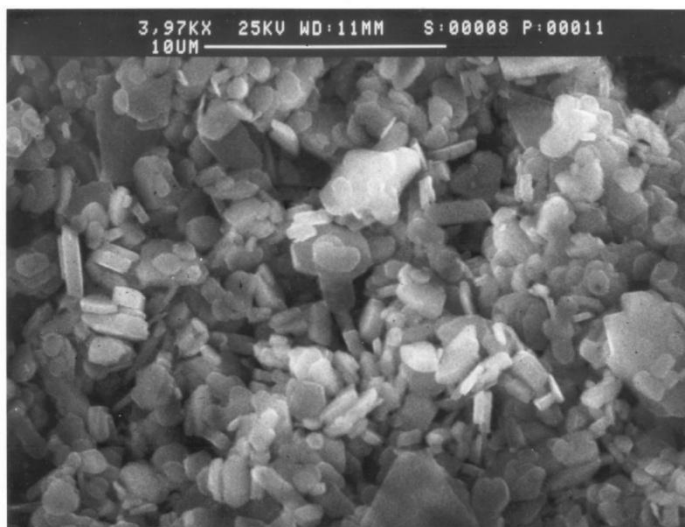


Figure 2: SEM micrograph of hydrated-micas obtained from the composition (*x* = 0.5) at 600°C, NNO and 1kbar.

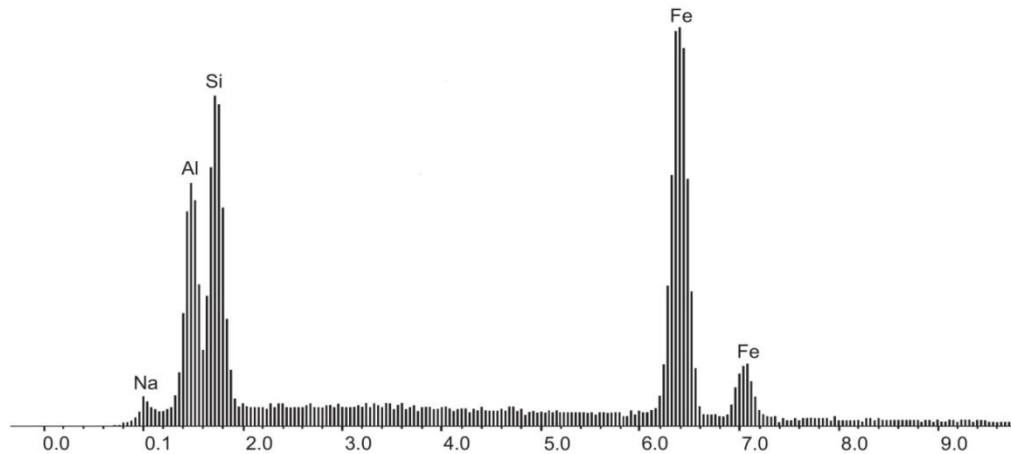


Figure 3: X-ray analysis spectra of the Na-Al annite(OH)(x = 0.5).

3.2. F-free MW buffered experiments

The run products of experiments performed at lower oxygen fugacity, 600°C and 1kbar, are listed in Table 2. The x = 0 starting composition (Na-annite end-member) produced fayalite and albite. The absence of any phyllosilicate phase at these conditions had already been noticed by [20] while [52] reported the synthesis of a “new” 10 Å trioctahedral mica end-member with the composition of Na-annite in the nepheline-silica-iron-oxygen-hydrogen system.

Table 2: Experimental products obtained at 600°C, MW buffer and 1kbar. Are also presented results of fluorinated compositions investigated at 600°C, NNO and 1kbar. (*) denotes those obtained at low oxygen fugacity by [20]. The phases encountered are Na-Al annite(F), mica <mc>, magnetite <Mag>, fayalite <Fay>, quartz <Qtz>, albite <Ab>, hercynite <Hcy>, montmorillonite <Mnt>, paragonite/montmorillonite <Pg/Mnt>, Na-annite <Na-Ann>, analcime <Anl>, expandible ordered mixed layer <eml>.

Starting composition	Phases obtained	Hydrates (Å)	T °C at PH ₂ O
F-free system: Present study			
(Na)(Fe ₃)(Si ₃ Al ₁)O ₁₀ (OH) ₂	Fay + Ab		600°C/MW/1kbar
(Na)(Fe _{2.5} Al _{0.5})(Si _{2.5} Al _{1.5})O ₁₀ (OH) ₂	eml + (Hcy)	2W = 14.891 1W = 11.339	600°C/MW/1kbar
(Na)(Fe ₂ Al ₁)(Si ₂ Al ₂)O ₁₀ (OH) ₂	mc + (Hcy)	2W = 15.021 1W = 11.832 0W = 9.831	600°C/MW/1kbar
F-free system : Results from [20]			
(Na)(Fe ₃)(Si ₃ Al ₁)O ₁₀ (OH) ₂	Na-Ann + Mnt + Fa + Anl	-	485°C/MW/5kbar
(Na)(Fe _{2.5} Al _{0.5})(Si _{2.5} Al _{1.5})O ₁₀ (OH) ₂	Na-Ann + mm + Pg/Mnt + Mag + Ab	-	500°C/MW/5kbar
(Na)(Fe ₂ Al ₁)(Si ₂ Al ₂)O ₁₀ (OH) ₂	mc + Hcy + (eml)	-	500°C/MW/5kbar
F-bearing system: Present study			
(Na)(Fe ₃)(Si ₃ Al ₁)O ₁₀ (F) ₂	mc + Mag + Qtz	0W = 9.645	600°/NNO/1kbar
(Na)(Fe _{2.5} Al _{0.5})(Si _{2.5} Al _{1.5})O ₁₀ (F) ₂	Na-Al annite(F)	0W = 10.045	600°/NNO/1kbar
(Na)(Fe ₂ Al ₁)(Si ₂ Al ₂)O ₁₀ (F) ₂	mc + (Hcy)	1W = 12.427 0W = 9.762	600°/NNO/1kbar

The experiments, for the nominal composition of Al-Na annite(OH) x = 0.5, yielded a hydrated layer mineral with 2W and 1W hydrates associated with hercynite. The XRD pattern of products obtained from Na-siderophyllite(OH) with x = 1.0 shows the presence of 2W and 1W hydrates, whose d₀₀₁ spacing are ~15.0 Å and ~11.8 Å, respectively. Minor amounts of anhydrous mica (0W) are also detected at this composition. The presence of the 0W mica phase is not clearly understood. It is

considered to be due to the lower Fe^{3+} content [53]. Fanz & Althaus [20] using the same magnetite iron (MI) buffer, obtained similar results, i.e. a polyphased assemblage, but with the presence of a montmorillonite/paragonite mixed layer mineral or a pure montmorillonite. The difference could be due to the lower temperature (500°C) used for their synthesis experiments.

3.3. F-bearing NNO buffered experiments

The runs whose starting composition was that of Na-annite(F) produced a mica phase associated with magnetite and quartz (Table 2). At the Na-Al annite(F) stoichiometry ($x = 0.5$) a pure single 0W mica with a high crystallinity was obtained, whereas the Na-siderophyllite(F) starting compositions ($x = 1.0$), produced a 0W mica phase associated with a small amount of 1W particles.

As expected, the XRD pattern of the Al-Na annite(F) run products show an intense 001 and higher-order (00*l*) reflections typical of the anhydrous state only (Fig. 4a).

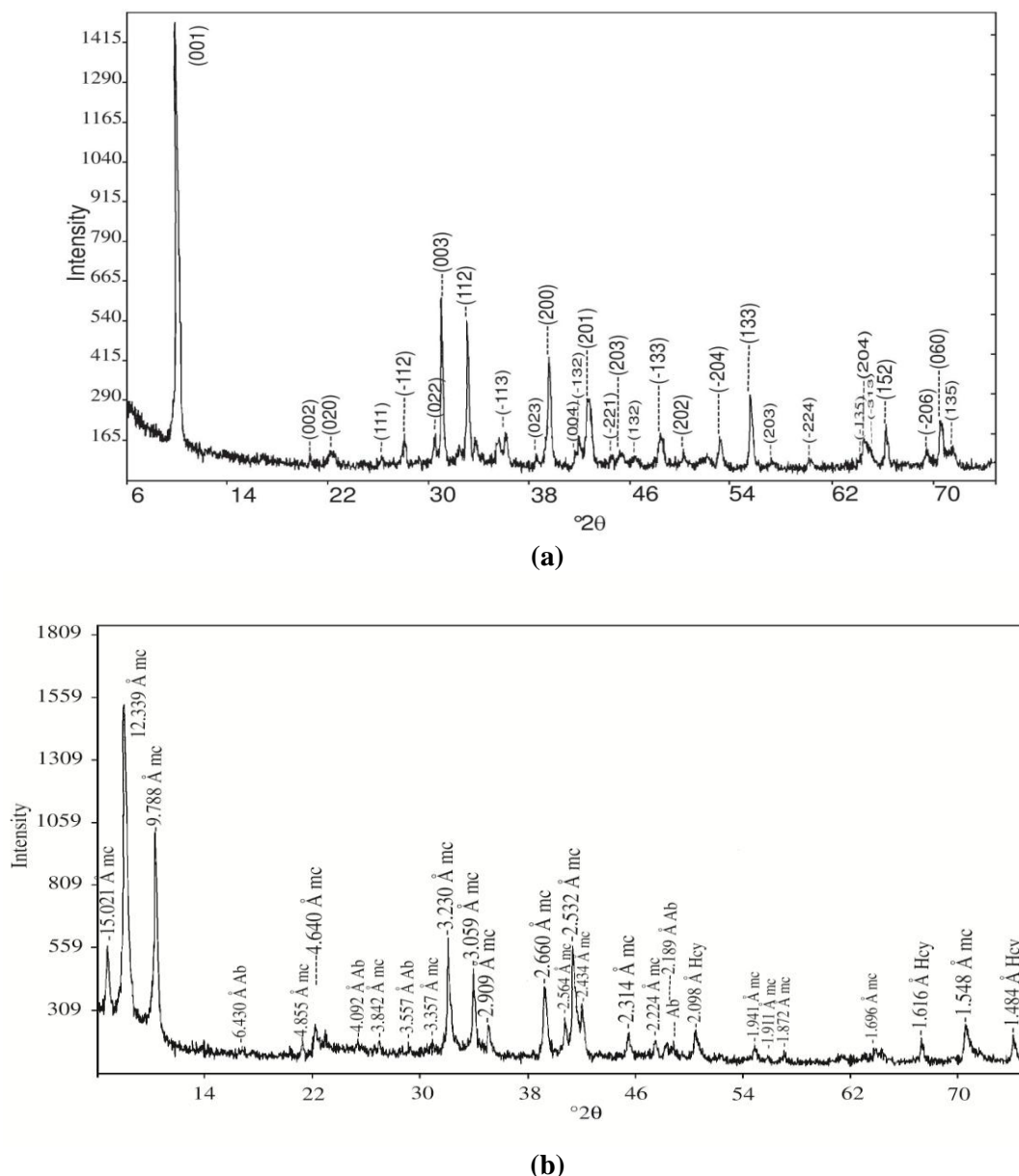


Figure 4: **a)** XRD pattern from randomly Na-Al annite(F) specimen obtained in the range $5\text{--}75^\circ 2\theta$. Indexing of peaks to the corresponding (hkl) reflections was done in accordance with the structure refinements of siderophyllite made by [50]. **b)** For comparison, XRD pattern corresponding to Na-Al annite(OH). The phases encountered are hydrated mica <mc>, albite <Ab>, hercynite <Hcy>.

The intensities of the diffraction peaks at 10.045 Å/001; 3.332 Å/003; 2.661 Å/200; 2.455 Å/201; 2.182 Å/-133; 1.915 Å/133; 1.547 Å/060 are 100%; 50%; 30%; 20%; 30%; 20% respectively, in agreement with the data reported for the same reflections measured on a natural K-Al annite(OH) specimen [49] and/or analogous synthetic products described by [50]. Furthermore, the weak line occurring at 5 Å and the peak at 1.55 Å, which corresponds to the d_{060} spacing, confirm the trioctahedral nature of this mica.

The most notable feature in our experiments is the contrasting behavior of F-bearing Na-micas, compared to their OH-bearing counterparts with the same cationic composition. F-bearing micas trap much less water in the interlayer than F-free ones (Fig. 4 a. b). The same feature had been already observed by [30] for synthetic hectorites.

3.4 Infrared spectra in the OH-stretching and lattice vibration regions

Selected powder FTIR patterns collected in the OH-stretching region on samples along the Na-Al annite(OH) - Na-siderophyllite obtained under NNO buffering conditions are displayed in Figure 5a. The run powder consisted of mica plus minor hercynite and analcime (Table 1), thus the absorption bands in the 4000-3000 cm^{-1} range are due to the mica phase only. The spectra shows a main broad absorption at 3640 cm^{-1} , with an evident shoulder at 3580 cm^{-1} , and the second, very broad absorption extending from 3500 to 3300 cm^{-1} . The first, most intense absorption can be decomposed into, at least, 4 component bands (Fig. 5b) which can be assigned on the basis of previous works relative to similar compositions [20].

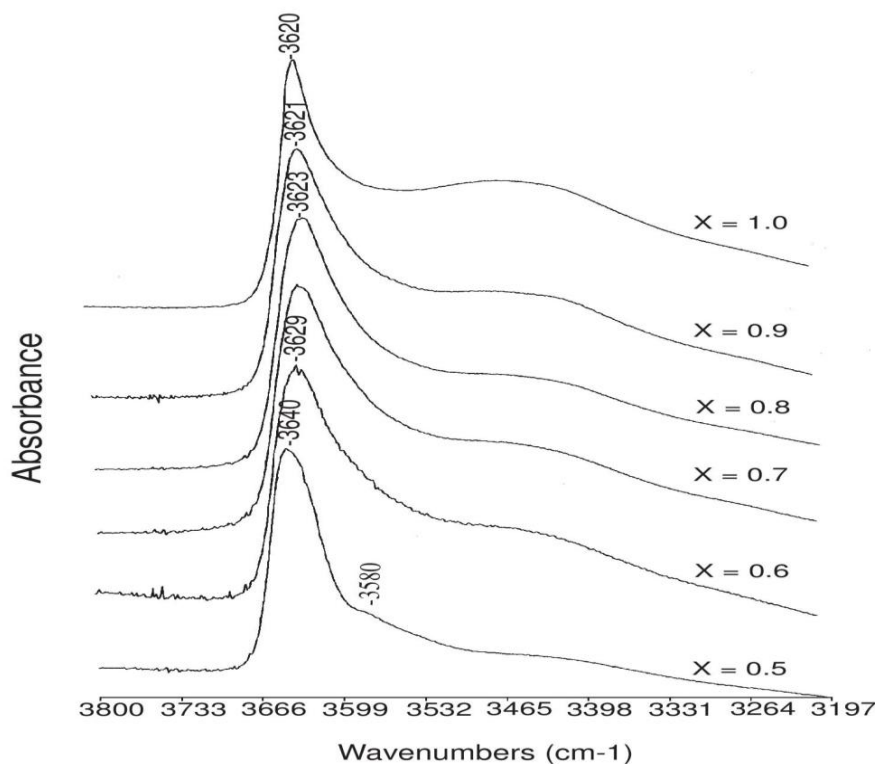


Figure 5a: Infrared absorption spectra as function of nominal $0.5 \leq x \leq 1$ in the OH-stretching vibrations region (3800–3200 cm^{-1}).

Accordingly, the higher frequency component resolved at 3640 cm^{-1} can be assigned to the stretching mode of OH groups bonded to three octahedrally coordinated Fe^{2+} cations. It is therefore a N-type band (Tri-6^+ : trioctahedral environment adjacent to six cationic charges). The second component is resolved at 3620 cm^{-1} , with a -20 cm^{-1} downward frequency shift with respect to the previous N-type band. Based on the controlled chemistry of the system, this shift can be assigned to the presence of Al ions close to the OH group, and thus the band can be classified as a I-type (impurity type) band, i.e. corresponding to the vibration of OH groups associated to ($\text{Fe}^{2+}\text{Fe}^{2+}\text{Al}^{3+}$) octahedral trimer. At lower wavenumbers (3600-3540 cm^{-1}), two broader absorption bands can

be resolved at 3590 cm^{-1} and 3540 cm^{-1} . Based on literature data, these values are characteristic of stretching vibrations of OH groups in dioctahedral environments. We thus assign the first band to vibrations of OH groups in $\text{OH-Fe}^{2+}\text{Al}^{3+}\square$ (Vb'), and the second band at 3540 cm^{-1} to the vibrations of OH-groups associated with $\text{Fe}^{3+}\text{Al}^{3+}\square$ octahedral environment Vb''. All these assignments are consistent with those reported for similar compositions along the K-annite-siderophyllite(OH) join, and therefore justified by the same arguments discussed here [20].

Considering that the spectra of Figure 5 have been collected on pellets dried overnight at 110°C , the broad absorption present in the $3500\text{-}3300\text{ cm}^{-1}$ range, besides reflecting the presence of minor residual moisture adsorbed on the pellet, can be confidently assigned to the presence of interlayer H_2O molecules in the sample. A final remark concerns the wavenumber shift ($10 - 15\text{ cm}^{-1}$) observed for the N-band between potassium and sodium series for the same tetrahedral starting composition. This effect can be partly due to the different electronegativities of Na and K ions; indeed, it is well known for the structurally closely related amphiboles where the presence of Na at the A-site induces the shift of the OH-stretching band of 5 cm^{-1} to lower frequency with respect to K [54-56]. However, this interpretation must be cautiously examined since the presence of Fe^{3+} substituting for Al^{3+} is also responsible for similar shifts. For instance, we observed a downward shift in wavenumber of $10 - 15\text{ cm}^{-1}$ for the N band caused by the substitution of $^{[4]}\text{Al}^{3+}$ by $^{[4]}\text{Fe}^{3+}$ in ferri-phlogopite.

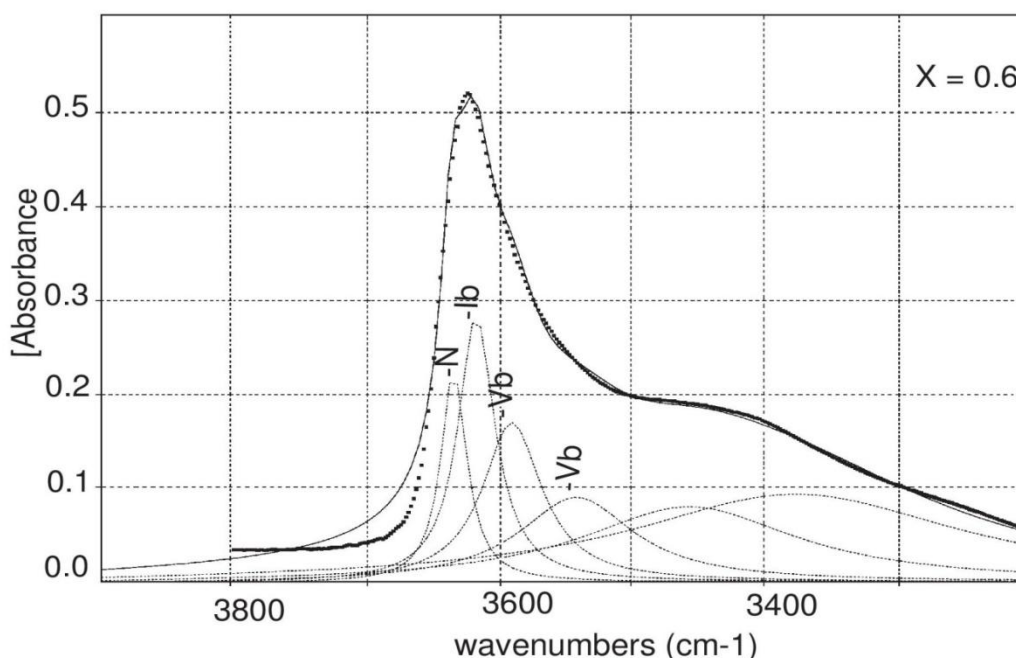


Figure 5b: Decomposed infrared spectrum of hydrated mica ($X = 0.6$) obtained at 600°C , NNO and 1kbar. N-band concerns OH bonded to 3Fe^{3+} ; Ib-band OH bonded to $\text{Fe}^{2+}\text{Fe}^{2+}\text{Al}^{3+}$; Vb OH bonded to $\text{Fe}^{2+}\text{Al}^{2+}\square$; Vb' OH-bonded to $\text{Fe}^{3+}\text{Al}^{3+}\square$.

In the region of lattice vibrations, the wavenumbers of most bands vary with the aluminum content. Two intense broad bands are observed around 993 and 473 cm^{-1} for the products obtained from starting composition corresponding to $x = 0.5$ (Fig. 6). On the basis of literature concerning similar compositions, they are assigned respectively to the antisymmetric Si-O-Si (Si-O//) stretching vibrations [transition moment roughly parallel (//) to the cleavage plane] and to the motions of octahedrally coordinated cations [20] and/or to Si-O vibrations coupled to octahedrally coordinated cations [58]. These two bands shift to higher wavenumbers as the aluminum content increases from $x = 0.5$ to $x = 1$. This effect suggests that the Si-O bond length decreases with the Tschermak-type substitution as a result of a higher distortion of the tetrahedra. These distortions are induced in Al-rich micas to compensate the charge deficit on the oxygen atoms resulting from the $^{[4]}\text{Si}^{4+} \rightarrow ^{[4]}\text{Al}^{3+}$. A well-defined shoulder on the low-frequency side of the 993 cm^{-1} main band is observed at $\sim 900\text{ cm}^{-1}$;

this component may be assigned to a Si-O stretching vibrations with the transition moment perpendicular \perp to the cleavage plane (001), as proposed by [59]. In the Na-Al annite(OH) spectrum, the low intensity band at 744 cm^{-1} has been assigned by [57] in K-mica to an Al-O (\perp) stretching vibration. As aluminum increases toward the Na-siderophyllite(OH) end member, this band splits into two components at 739 and 797 cm^{-1} . The same split affecting the Si-O-Al bands (at ~ 641 and 657 cm^{-1}) at the expense of the Si-O-Si ones which occurs at $\sim 660\text{ cm}^{-1}$ has been observed in the spectra along the potassic annite-siderophyllite series. Finally, the band at 570 cm^{-1} in the Na-Al annite(OH) spectrum, which is assigned by [57] to OH-vibrations, shifts to lower wavenumbers with increasing Al content.

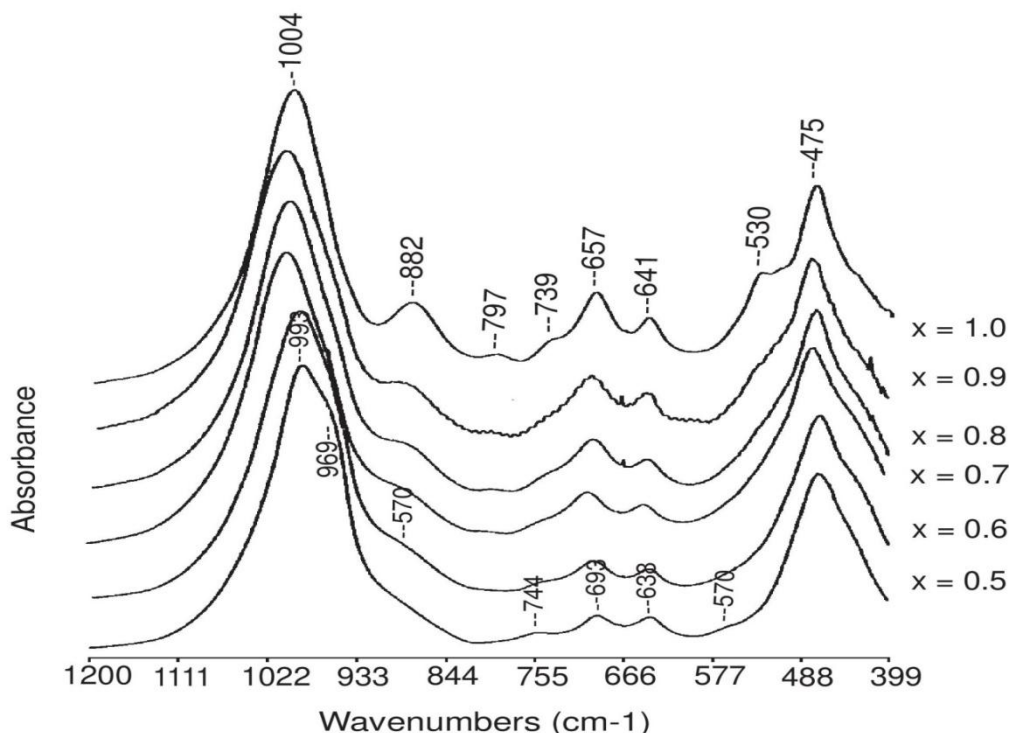


Figure 6: Infrared absorption spectra as function of nominal $0.5 \leq x \leq 1$ in the lattice vibrations region ($1400\text{--}400\text{ cm}^{-1}$).

3.5 Discussion

In Fluorine-free system, no purely anhydrous micas have been obtained along the Na-annite-siderophyllite(OH) join, whatever the temperature and redox synthesis conditions. The highest amount of 0W mica is formed in oxidizing conditions, under the NNO buffer at 600°C and 1 kbar. The run products always contained a mixture of the hydrated states described by [48]. According to X-ray diffraction data, the highest amount of the hydrated mica phase has been obtained for the Na-Al annite(OH) stoichiometry, suggesting that crystallization is promoted by the presence of trivalent cations (Al^{3+} and Fe^{3+}). This is particularly the case for Fe^{3+} ions which is present in the mica phase, as shown by the Mössbauer measurements [59,60] and indicated by the FTIR data discussed above. The infrared spectra of the synthesized micas outline the heterogeneous nature of the octahedral sheets, where trioctahedral local configurations coexist with dioctahedral ones and where Fe^{3+} and Al^{3+} ions are present in the octahedral sites. The amount of the obtained mica phase at the Na-siderophyllite(OH) stoichiometry is comparatively lower: the 2W hydrated layers disappear. The predominant state of the mica is the one-layer hydrateone. This can be explained considering that increasing tetrahedral $\text{Si}^{4+} \rightarrow \text{Al}^{3+}$ substitution in Na micas reduces the possibility for the interlayer expansion [61] and consequently for the hydration property.

According to numerous authors [e.g. 62-65], the hydration state of phyllosilicates depends both on their chemical composition and on the ambient humidity. The hydrated micas obtained from Na-Al annite(OH), exhibit the three hydrated states. Such a feature can be regarded as the result of the distribution of intra and inter-layer charge deficits. However, it is important to emphasize the structural contribution and the role played by water in the relative stability of Na-micas. Considering K-annite(OH), the ionic radius of potassium is 1.64 Å in 12-fold coordination (values from [66]). The alkali site is wide due to a little dimensional misfit which exists between the octahedral and tetrahedral sheets on one hand, and the tetragonal rotation angle α (1.5°) close to 0° [51] on the other hand. Besides, due to its ionic radius (1.39 Å and 1.02 Å in 12- or 6- fold coordination, respectively) lower than that of potassium, Na may fit only in sufficiently closed interlayer sites. For this reason the Na equivalent of K-annite(OH) cannot be stable, contrarily to the conclusions of [21]. Thus, our results are consistent with those obtained by [18], [67] and [68] who showed that the geometry of the alkali site is largely controlled by the composition of the tetrahedral and octahedral layers. These parameters control the geometrical fit between the structural units and consequently the tetrahedral rotation angle, which ultimately affects the dimension of the alkali site. Accordingly the alkali site has its maximum closure at the Na-siderophyllite(OH) composition. Consequently, only one molecule of water per sodium is sufficient to achieve the stable structural configuration.

All compositions investigated in the fluorine-bearing system produced a high content of 0W mica with very small amounts of mono-hydrated layers (1W). The OH → F substitution stabilizes the trioctahedral mica as shown by several previous works [69-72]. Indeed, the substitution of F in the structure induces structural adjustments which make the sodium ions to fit exactly into the interlayer site as proposed by [73]. The elimination of the Na⁺-H⁺ repulsion induces a reduction of the interlayer space, and, consequently, its capacity to trap water molecules. The positive charge of Na⁺ ion is equally distributed over all the surrounding oxygens, stabilizing the local charge configuration. Thus, the hydration capacity is reduced but not cancelled [30] and by [73] for the K-biotite(OH, F) series. The solubility of fluorine in the examined system appears to be more extensive for the Na-Al annite(F) composition. This behavior, already noted for potassium equivalents along the join K-annite-siderophyllite (OH, F) join, could be explained by structural similarities between annite and eastonite [43; 73].

Fluorine is actively involved in mineralization process, as suggested by several studies on biotites coexisting with (OH,F)-fluids [32-35]. Experimental investigations performed on biotites in equilibrium with alkali fluids resulted in incipient instability of the phyllosilicate phase with the formation of new minerals which incorporate ore-forming elements [74]. The results we present suggests that, when studying geological samples from occurrences where F-enriched fluids may have played a role, a detailed crystal-chemical characterization of phyllosilicates is needed through modern instrumental techniques, because of the possibility to confuse early crystallization with alteration phases.

The Na hydrated micas obtained in Fluorine-bearing and in Fluorine-free system are not phyllosilicates as those resulting from the alteration of pre-existing minerals, but may be regarded as primary water-rich sodic phyllosilicates obtained under relatively high temperature and pressure conditions. This conclusion is in agreement with the important findings of [22] who described sodic biotites in prograde metamorphic schists from the betic cordilleras (Spain).

Conclusion

1. The data obtained in this study for the F-free system, are in general agreement with earlier experimental works [17-20]. As a matter of fact, we did not obtain pure single anhydrous sodium micas (0W) in the experimental conditions imposed here. The Na equivalent of K-annite(OH) cannot be stable, the geometry of the alkali site is largely controlled by the composition of the tetrahedral and octahedral layers. However, at oxidizing conditions buffered by NNO, significant amounts of hydrated mica have been obtained under relatively high temperature and pressure conditions.

2. The presence of fluorine allowed the formation of an almost monophasic run product composed of a sodium mica, with high crystallinity along the joint annite(F)-siderophyllite(F). Na-Al annite(F) is synthesized under moderate hydrothermal conditions (600°C, NNO buffer and 1kbar). It's a promising compound which must be of a fine crystal-investigation.
3. Indeed, the Na hydrated micas obtained during the present work are not as those resulting from the alteration of pre-existing minerals, but may be regarded as primary water-rich sodic phyllosilicates.
4. It should be noted that the substitution of fluorine in Na-mica, could have interesting technical applications, including for example the possibility to use these materials for the removal of fluorine, metals and organic compounds from the solutions.

Acknowledgements - I remain indebted to CRSCM that allowed me to do all the experiments carried out in this work: CRSCM-CNRS, France. I want to thank Pr. Ruiz Cruz, M.D for corrections she made to the manuscript and also Ph.D Amel for bibliographic assistance it has given to this work.

References

1. Guidotti C.V., *Rev Mineral*, Bailey SW (ed), 13 (Eds) (1984) 357-467.
2. Dymek R.F., *Am Mineral*. 68 (1983) 880-899.
3. Deer W.A., Howie, R.A., Zussman, J., *Rock Forming Minerals*. Longman, London, 3 (Eds) (1962) 270 pp.
4. Franz G., Althaus, E., *Neues Jahrb Mineral Abh.* 126 (1976) 233-253.
5. Peng G.Y., Lewis, J., Lipin, B., Mc Gee, J., Bao, P.S., Wang X.B., *Am Mineral*. 80 (1995) 1307-1316.
6. Cabella R., Gazzotti M., Luccetti, G., *Can Mineral*. 35 (1997) 899-908.
7. Melcher F., Grum, W., Simon, G., Thalhammer, T.V., Stumpf, E.F., *J Petrol*. 38 (1997) 1419-1458.
8. Yang J.J., Jahn, B.M., *J M Geol*. 18 (2000) 167-180.
9. Keusen H.R., Peters, T.J., *Am Mineral*. 65 (1980) 1134-1137.
10. Meyer J., *Terra Cognita*, 3 (1983) 187.
11. Godard C.G., Smith, D.C., 10^{ème} R.S.T, (1983), Bordeaux. France.
12. Godard C.G., Smith, D.C., *Contrib Mineral Petr.* 136 (1999) 20-32.
13. Dempster T.J., Jackson, R.A., *Sc. J. Geol.* 32 (1969) 173-177.
14. Ruiz Cruz M.D., Novak, J., *Eur. J. Mineral*. 15 (2003) 67-80.
15. Spear F.S., Hazen, R.M., Rumble, D., *Am Mineral*. 66 (1981) 100-105.
16. Veblen D.R., *Am Mineral*. 68 (1983) 554-556.
17. Hewitt D.A., Wones, D, *Am Mineral*. 60 (1975) 854-862.
18. Rutherford M.J., *J Petrol*. 10 (1969) 381-408.
19. Franz G., Althaus, E., *Contrib Mineral Petr.* 46 (1974) 227-232.
20. Franz G., Althaus, E., *Neues Jahrb Mineral Abh.* 126 (1976) 233-253.
21. Weidner I.R., Carman, H.P., *Geological Society of America*, Abst., 81st Annual Meet, (1968) 314-315.
22. Ruiz Cruz M.D., *Clay Clay Miner.* 52 (2004) 603-612.
23. Schreyer W., Abraham, K., Kulke, H., *Contrib Mineral Petr.* 74 (1980) 223-233.
24. Komarneni S., Pidugu, R., Hoffbauer, W., Schneider, H., *Clay Clay Miner.* 47 (1999) 410-416.
25. Chipera J.S., Bish, L.D., *Clay Clay Miner.* 50 (2002) 38-48.
26. Toksoy-Koksal Fatma., Turkmenoglu A.G., Goncuoglu, M.C., *Clay Clay Miner.* 49 (2001) 81-91.
27. Banno Y., Miyawaki, R., Kogure, T., Matsubara, S., Kamiya, T., Yamada, S., *Mineral Mag.* 69 (2005) 1047-1057.
28. Melka K., Ulrych, J., Mikulas, R., *Acta-Geodyn-Geomater.* 2 (2005) 119-129.
29. Pavón E., Castro, M.A., Naranjo, M., Mar Orta, M., Pazos, M.C., Alba, M.D., *Am Mineral*. 98 (2013) 394-400.
30. Dazas B., Lanson, B., Breu, J., Robert, J.-L., Pelletier, M., Ferrage, E., *Micropor Mesopor Mat.* 181 (2013) 233-247.
31. Tischendorf G., *Inst. Min. Metall.*, Sect. B82 (1973) B7-24.
32. Zaw K., Clark, A.H., *Can Mineral*. 16 (1978) 207-221.

33. Parry WT., Ballantyne, G.H., Wilson, J.C., *Econ. Geol.* 73 (1978) 1308-1314.
34. Gunow A.J., Ludington, S. Munoz, J.L., *Econ. Geol.* 75 (1980) 1127-1137.
35. Imeokparia E.G., *J. Min. Geol.* 18 (1981) 198-203.
36. Josephus Thomas JR., Glass, H.D., White, W.A., Trandel, R.M; *Clay Clay Miner.* 25 (1979) 278-284.
37. Majid A., Argue, S., Kingston, D., Lang, S., *J Fluorine Chem.* 128 (2007) 1012-1018.
38. Hamilton D.L., Henderson, C.B.M., *Mineral Mag.* 36 (1968) 632-838.
39. Rieder M., Cavazzini, G., D'yakonov, Y.S., Frank-Kamentskii, V.A., Gottardi, G., Guggenheim S., Koval P.V., Müller G., Neiva, A.M.R., Radoslovich, E.W., Robert, J.-L., Sassi, F.P., Takeda, H., Weiss Z., Wones, D.R., *Clay Clay Miner.* 46 (1998) 586-595.
40. Wones D.R., Eugster H.P., *Am Mineral.* 50 (1965) 1228-1272.
41. Rutherford M.J., *J Petrol.* 14 (1973) 159-180.
42. Eugster H.P., *J. Chem. Phys.* 26 (1957) 1760-1761.
43. Boukili B., Holtz, F., Bény, J.-M., Robert, J.-L., *Schweiz Mineral Petrogr Mitt.* 82 (2002) 549-559.
44. Christanssen C., *Wiedemann Annalen der Physik und Chemie.* 23 (1884) 298-306.
45. Vedder W., *Am Mineral.* 49 (1964) 736-768.
46. Robert J.-L., Kodama, H., *Can Mineral.* 27 (1989) 225-235.
47. Boukili B., Holtz, F., Robert J.-L., Jorion, M., Bény, J.-M., Naji, M., *Schweiz Mineral Petrogr Mitt.* 83 (2003) 33-46.
48. Carman J.H., *Am Mineral.* 59 (1974) 261-273.
49. Gottesmann B., *Geologie.* 11 (1962) 1164-1176.
50. Redhammer G.J., Beran, A., Schneider, J., Amthauer, G., Lotthermoser, W., *Am Mineral.* 85 (2000) 449-465.
51. Hazen R.M., Burnham, C.W., *Am Mineral.* 58 (1973) 889-900.
52. Weidner I.R., Carman, H.P., Geological Society of America, Abst., 81st Annual Meet, (1968) 314-315.
53. Hoda S N., Hood, WC., *Clay Clay Miner.* 20 (1972) 343-358.
54. Robert J.-L., Della Ventura, G., Thauvin, J. L., *Eur. J. Mineral.* 1 (1989) 203-211.
55. Della Ventura, G., *Trends in Mineralogy.* 1 (1992) 153-192.
56. Hawthorne, F.C., Della Ventura, G., *Rev. Mineral*, Bailey SW (ed), 67 (2007) 173-222.
57. Farmer, V.C., *The infrared spectra of minerals* (Farmer, V.C, editor). Society of London. (Eds) (1974) 331-363.
58. Jenkins, M.J., *Phys Chem Miner.* 16 (1989) 408-414.
58. Ishii, M., Shimanouchi, T., Nakahira, M., *Inorg. Chim. Acta.* 1 (1967) 387-392.
59. Boukili B., Thèse, Univ. Orléans, France, (1995) 320 pp.
60. Kitajima K., Daimon, N., Kondo, R., *Clay Miner.* 13 (1978) 167-175.
61. Moore D. M., Hower, J., *Clay Clay Miner.* 34 (1986) 379-384.
62. Watanabe T., Sato, T., *Appl. Clay Sci.* 7 (1988) 129-138.
63. Yamada H., Nakazawa, H., Hashizume, H., Shimomura, S., Watanabe, T., *Clay Clay Miner.* 42 (1994) 77-80.
64. Laird A.D., *Clay Clay Miner.* 47 (1999) 630-636.
65. Shannon R.D., *Acta Crystallgr.* A32 (1976) 751-767.
66. McCauley J.W., Newnham, R.E., *Am Mineral.* 56 (1971) 1626-1637.
67. Liu X., Thèse de 3^{ème} cycle, Univ. Orléans, France, (1989) 105 pp.
68. Munoz J.L., Ludington, S.D., *Am J Sci.* 274 (1979) 396-413.
69. Munoz J.L., *Rev. Mineral*, Bailey SW (ed), 13 (Eds) (1984) Pp 469-493.
70. Mason R.A., *Can Mineral.* 30 (1992) 343-354.
71. Robert J.-L., Bény, J.-M., Della Ventura, G., Hardy, M., *Eur. J. Mineral.* 5 (1993) 7-18.
72. Boukili B., Robert, J.-L., Beny, J.-M., Holtz, F., *Schweiz Mineral Petrogr Mitt* 81 (2001) 55-67.
73. Yu Yunmei., Wang Y., *Chin. J. Geochem.* 7 (1988) 76-87.